# **Absolut Modelica library**

Carles Ribas Tugores<sup>1</sup> Gerald Zotter<sup>1</sup> Carina Seidnitzer-Gallien<sup>1</sup>

<sup>1</sup>AEE - Institute for Sustainable Technologies, Feldgasse 19, Gleisdorf, 8200, Austria, {c.ribastugores, g.zotter, c.seidnitzer-gallien}@aee.at

#### **Abstract**

This publication presents a Modelica library developed to investigate absorption thermodynamic cycles, with special attention to the absorption heat exchanger (AHE). The library includes models for different absorption cycles at various levels of detail, most of which have been validated against literature values. The AHE concept and the main components used to develop a dynamic AHE model, together with validation results based on laboratory measurements, are described in detail. The library is available at https://github.com/carlesRT/Absolut.

Keywords: Modelica library, Absorption thermodynamic cycles, Absorption heat exchanger, H<sub>2</sub>O/LiBr

### 1 Introduction

## 1.1 The absorption heat exchanger

The absorption heat exchanger (AHE) concept involves the integration of an absorption heat pump (AHP) with a conventional heat exchanger (HEX), see Figure 1. The main advantage of this configuration is the lower return temperatures achieved on the primary (hot) side compared to standard solutions, such as water-water counterflow heat exchangers. The AHE concept was originally introduced and discussed in (Fu et al. 2010), (Li et al. 2011) and (Yin Zhang, Shi, and Yinping Zhang 2014).

The primary supply stream at temperature  $T_{11}$  first passes through the generator, where it provides heat to produce the refrigerant vapor. It then enters the external heat exchanger, and subsequently flows into the evaporator, where it can be cooled to a temperature lower than the secondary return temperature ( $T_{12} < T_{22}$ ). On the secondary side, the return stream is heated by the external heat exchanger, the absorber, and the condenser. Various configurations are possible (e.g. absorber, condenser and HEX arranged in parallel). In the configuration shown in Figure 1, the secondary stream is split into two branches; one flows through the external heat exchanger, while the other passes through the absorber and then the condenser.

The AHE concept is applied mainly in China, with a notable project located in Taiyuan-Gujiao, China (Hu, Jiang, and Xie 2009). In this project, an AHE is integrated into a 50 km long district heating line connecting a CHP plant to the city center to increase heat transport capacity. Through this integration, the system can deliver 3.2 GW of heat at 130°C/20°C, demonstrating the significant reduction in

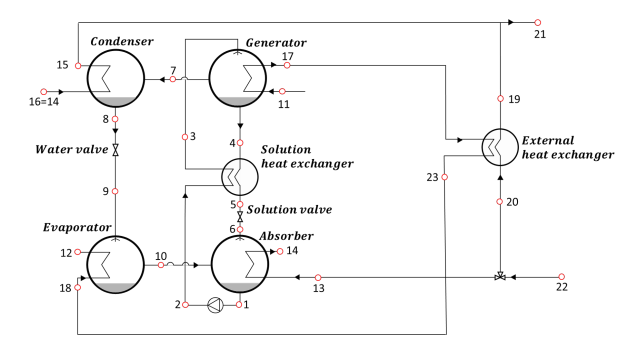


**Figure 1.** Schematics of an absorption heat exchanger. Numbers indicate the positions of referenced variables.

return temperature achievable with this technology. Interest in the AHE concept within the district heating sector is also growing in Europe (G. Beckmann, F. Schittl, G. Piringer, D. Rixrath, R. Krotil, J. Krail 2019; Yang, Mirl, and Schmid 2020; Zotter, Eberhöfer, and Seidnitzer-Gallien 2023).

## 1.2 Open-Source Modelica models

The modeling language Modelica (Modelica Association n.d.) was selected to develop the necessary models for conducting various studies within the Absolut project and upcoming studies on future energy concepts within the TREASURE<sup>1</sup> project.

Before initiating the modeling process, a literature review was conducted, which included testing available open-source models, to assess their suitability for the planned work. Commercial libraries such as TIL (*TIL Suite* n.d.) and in-house models (e.g. (Cudok 2021; Corrales Ciganda et al. 2016; De La Calle et al. 2016; Wernhart et al. 2022)) were excluded from this review. The review identified three primary libraries. The key findings are summarized in Appendix A.

The review of open-source models for absorption machines yields the following conclusions.

Compatibility with other Modelica libraries: The use
of standardized interfaces (e.g. fluidPort) enables
a modeling approach that leverages validated models
from multiple sources and facilitate interoperability.
This approach has been adopted by the authors to enhance the usability of their models within the broader
Modelica ecosystem.

<sup>&</sup>lt;sup>1</sup>TREASURE project: www.treasure-project.eu

- Object-oriented modeling approach: The DCOL library (Febres et al. 2017) adopts an object-oriented approach, with separate models for key components (e.g. absorber, generator), which supports modularity, ease of development, and maintainability. The same approach is followed in this work, with DCOL models serving as a reference for the implementation of the dynamic models.
- Initialization Challenges: Some evaluated models encountered difficulties during initialization and execution, highlighting the importance of a robust model structure and well-defined initial values to improve usability. The models developed in this work include runnable examples, which also serve as a reference for troubleshooting newly created or modified models.
- Fluid Property Implementation: Although fluid property correlations are available, inconsistencies in their implementation may lead to numerical instabilities. Existing libraries would benefit from a more consistent and reliable representation of fluid properties.

#### 1.3 The Absolut library

A wide range of models at varying levels of complexity has been implemented. Given the number of Modelica models publicly available compared to those described in the literature (see section 1.2), we believe that the open-source community can benefit from this contribution. The provided library offers a reliable set of simplified models suitable for case studies or as a foundation for further development. However, it should be noted that the implementation work was primarily focused on the dynamic modeling of the absorption heat exchanger (AHE).

The Absolut library includes models for absorption heat pumps at three main levels of detail: basic (zero-order), static, and dynamic models. The left side of Figure 2 provides a view of the main package structure. Most of the models have been validated using examples from (Herold, Radermacher, and Klein 2016). The static and dynamic models use H<sub>2</sub>O/LiBr as the working pair, for which thermophysical correlations have been implemented (see section 2.2). The use of alternative working pairs is subject to two main conditions: first, the compatibility between the models and the implemented fluid property correlations; and second, the validity of the model assumptions (e.g., the assumption of a pure refrigerant at the generator outlet). Mention that some modifications will be most likely required due to the use of some non-standard functions such as temperature\_Xp() on the mixture side (H<sub>2</sub>O/LiBr). These can be addressed by adding missing functions to the new working pair package or better adapting the models to use more standardized functions, e.g. temperature (setDewState()). Similar compatibility issues might also arise on components using purerefrigerant.

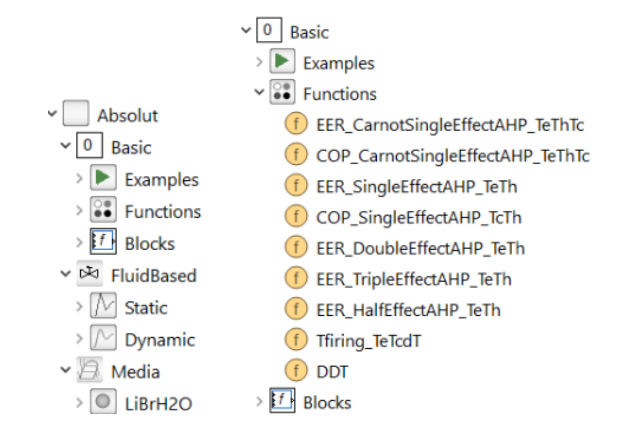


**Figure 2.** Overview of main packages structure (left) and Basic package (right).

Usability has been confirmed primarily in Dymola (*Dymola* 2024), with partial testing performed in OpenModelica (*OpenModelica* 2024) to ensure usability with purely open-source environment.

# **2** Description of models

#### 2.1 Ideal models

The Basic package contains models based on an idealized representation of the thermodynamic cycle for absorption machines. The core models are implemented as functions, which are encapsulated in blocks with input/output interfaces to facilitate their use via the graphical user interface. All the available functions are shown in the right side of Figure 2. The application of these functions and blocks is demonstrated through several examples.

The provided examples are adapted from (Herold, Radermacher, and Klein 2016) and are used to verify the correctness of the implementation. In addition, .mos scripts are included with each example to facilitate automated simulation and visualization of results.

Most of the models included in the Basic package are based on the Carnot cycle (reversible pro-By combining the Carnot cycle for power generation with a refrigeration cycle, the efficiency of a single effect absorption heat pump can be derived. This principle forms the basis of the functions EER\_CarnotSingleEffectAHP\_TeThTc and COP\_CarnotSingleEffectAHP\_TeThTc, as well as their corresponding blocks. The Carnot-based functions are further refined to account for the primary source of irreversibility in absorption cycles, which is associated with heat transfer between the cycle and its surroundings (Herold, Radermacher, and Klein 2016). This refinement is achieved by introducing a thermal resistance between the external and internal temperatures, resulting in a temperature difference. It is important to note that the internal cycle of the AHP is still assumed to be reversible. This assumption, along with the assumption that the temperature difference between the condenser and the generator is equal to that between the condenser and the evaporator, forms the basis of the so-called zero-order model (Herold, Radermacher, and Klein 2016). This models is used to derive the functions EER\_SingleEffectAHP\_TeTh and COP\_SingleEffectAHP\_TeTh to calculate the cooling and heating efficiency respectively of a single effect absorption heat pump. Similar functions are implemented to calculate the cooling efficiency of double effect, triple effect and half effect absorption heat pumps.

The main practical application of the basic models is to quickly estimate the expected efficiency and thereby the feasibility - of an absorption cycle Conversely, they for given operating temperatures. can be used to estimate the required driving temperature needed to deliver heat at a target temperature Absolut.Basic.Blocks.Tfiring). that the use of input/output interfaces is in line with the intended use of the models. However, this approach restricts the use of the blocks, as, for example, EER\_CarnotSingleEffectAHP cannot be used to determine the driving temperature Th given the desired efficiency (EER) and the temperatures Tc and Te. Nevertheless, this result can be obtained by using the function EER\_CarnotSingleEffectAHP\_TeThTc directly, as both Dymola and OpenModelica are capable of interpreting and manipulating the function to solve for the input temperature Th.

#### 2.2 Fluid properties

The static and dynamic models use pure water as a refrigerant, specifically employing the implementation based on the IAPWS/IF97 standard provided in the Modelica Standard Library (MSL) (Modelica Association 2024). The thermodynamic correlation for the working pair H<sub>2</sub>O/LiBr is based on the formulation from (Yuan and Herold 2005) and has been implemented in Modelica.

This correlation follows a global approach to ensure improved consistency across properties. Rather than fitting individual thermodynamic properties separately, a fundamental function - in this case Gibbs free energy - is selected. All relevant properties are derived from this function using thermodynamic relationships (e.g. entropy is obtained from the partial derivative with respect to the temperature of the Gibbs free energy). The correlation expresses the Gibbs free energy as a function of temperature, pressure, and lithium bromide mass fraction. All available thermodynamic data are then used simultaneously to determine the main coefficients of the fundamental function. The correlation obtained gives good accuracy over the full range of liquid concentrations from pure water up to the crystallization line and from 5°C to 250°C (Yuan and Herold 2005). Examples verifying the implementation are included in the Media.LiBrH2O.Validation package.

#### 2.3 Static models

The ...FluidBased.Static package contains models for components such as valves, pumps, primary heat exchangers (absorber, generator, evaporator, and condenser) and solution heat exchangers. These component models can be combined to assemble various thermodynamic absorption cycles.

Several cycle configurations have already been implemented, including single effect and double effect absorption heat pumps (AHP), absorption heat transformer (Type II AHP), absorption heat exchanger (AHE) and resorption cycle. In some cases, multiple variants of a given cycle are provided, for example AHE model with the absorber and condenser arranged in parallel, and a version with all flows in parallel. These models can be used to roughly assess the required size, or better said the required UA value, for a given application (temperatures, heating capacity, configuration), while disregarding process dynamics. As a result, their use is limited when analyzing control strategies.

Most of the models implemented have been verified using examples from (Herold, Radermacher, and Klein 2016). The corresponding verification models are included in the respective Validation packages. Some results are included in Appendix B.

#### 2.3.1 Heat exchangers

A detailed description of the main heat exchanger models (evaporator, etc.) is omitted here, and only a few remarks are provided on the available models.

All primary heat exchangers, and consequently the thermodynamic absorption cycles, are modeled using the standard fluidPort interface for external fluid connections. This allows the models to be integrated with their respective heat sources and sinks. However, for the single effect absorption heat pump, simplified versions of the models are also provided without a heat exchanger (Static.SingleEffect\_intern). These omit the external fluid interfaces and are intended for simulations under prescribed operating conditions (e.g. given pressure and LiBr concentration at the generator and absorber) that can be used to easily evaluate a prescribed thermodynamic cycle and to provide reference values for initializing more complex models.

Models that consider the heat exchanger and have fluidPort interfaces calculate the total heat transfer using the commonly applied simplified method, which is based on the product of the overall heat transfer coefficient (UA) and the logarithmic mean temperature difference (LMTD), as described in (Herold, Radermacher, and Klein 2016). As the calculation of LMTD might be problematic, the NoEvent operator is included to avoid division by zero. Furthermore, the approximation of the LMTD proposed by Chen (Chen 1987) is also implemented, see ...Static.BaseClasses. As reported in Petterson (Pettersson 2008) the deviation between the LMTD and Chen expression is very small. Either the LMTD method or Chen's approximation can be selected,

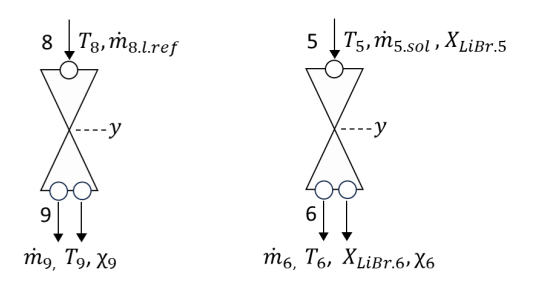


**Figure 3.** Schematics of the valve model: Refrigerant side (left) and solution side (right).

with LMTD used as the default.

Some relevant limitations and weak points of the current implementation, in addition to the fact that the models are static, includes the use of constant UA values (defined as parameters) and the limited use of extends clause, which leads to code duplication and consequently increases the risk of errors and maintenance effort.

Additionally, three heat exchanger models from the Buildings library, PartialEffectivenessNTU, PlateHeatExchangerEffectivenessNTU and ConstantEffectiveness, have been incorporated into the library using the extends clause package ... Static.Components.HEX). additional parameter has been introduced to later facilitate model substitution via the redeclare keyword. In the context of the static models, these models are intended to be used to model the solution heat exchanger. The simplest ones are simpleHX, which extends PartialEffectivenessNTU and fixes the UA value, and ConstantEffectiveness which assumes а constant effectiveness. PlateHeatExchangerEffectivenessNTU is more complex model with a variable UA value.

#### **2.3.2** Valves

Both the solution valve and the refrigerant valve are modeled assuming isenthalpic expansion and with no mass accumulation. The incoming fluid may undergo flashing, therefore the valve model calculates the outlet vapor quality,  $\chi$ , defined as the mass fraction of vapor at the outlet. State points are numbered for ease specific location in the system, see Figure 3. Additionally, subscripts are used to further specify variables, as detailed in the nomenclature section. Subscripts are separated by a dot. For flow related variables (e.g. mass flow rate), a positive value indicates inflow into the component, while a negative value indicates outflow. This sign convention has already been incorporated into the governing equations, consequently, flow variables should be considered in terms of their absolute values. The common mass and energy balance equations for the refrigerant and solution valve are:

$$0 = \dot{m}_i - \dot{m}_k$$
 where  $(j,k) \in \{(8,9), (5,6)\}$ 

$$\chi_j = \frac{\dot{m}_{j,\nu}}{\dot{m}_j} \quad \text{where } j \in \{9,6\}$$
 (2)

$$h_j = (1 - \chi_j) \cdot h_{j,l} + \chi_j \cdot h_{j,v}$$
 where  $j \in \{9,6\}$  (3)

An additional mass balance equation for lithium bromide is required for the solution valve,

$$0 = \dot{m}_{5,l,sol} \cdot X_{LiBr,5} - \dot{m}_{6,l,sol} \cdot X_{LiBr,6} \tag{4}$$

The mass flow rate is determined by Equations (5) and (6). It is modeled as being proportional to the valve opening signal y, the pressure difference across the valve, and a constant based on nominal operating conditions. Specifically, the nominal mass flow rate  $\dot{m}_{nom}$  is defined for a fully open valve (y=1) and a specified nominal pressure difference  $dp_{nom}$ . The pressure levels correspond to the pressures in the respective vessels. For example, in the case of the refrigerant valve, the pressure difference is calculated using the pressure in the condenser  $p_c$  (position 8) and the pressure in the evaporator  $p_e$  (position 9).

$$\dot{m}_{8.l} = y \cdot (p_c - p_e) \cdot \frac{\dot{m}_{nom}}{dp_{nom}} \tag{5}$$

$$\dot{m}_{5.l} = y \cdot (p_g - p_a) \cdot \frac{\dot{m}_{nom}}{dp_{nom}} \tag{6}$$

#### **2.3.3** Pumps

Equation (7) used to obtain the electrical power consumption of the solution pump  $W_{el}$  is obtained assuming incompressible flow and isentropic compression. It is defined as the ratio of the hydraulic work  $W_h$ , to the pump efficiency  $\eta$ . The hydraulic work is determined as the product of the mass flow rate at the pump inlet, the specific volume  $\nu$ , and the pressure difference between outlet and inlet. For a single effect AHP, this pressure difference corresponds to the pressure at the generator (high pressure) and the absorber (low pressure).

$$W_{el} = \frac{W_h}{\eta} = \frac{(p_g - p_a) \cdot \mathbf{v} \cdot \dot{m}_{1.l}}{\eta} \tag{7}$$

The hydraulic work is added to the fluid as an enthalpy increase. Fluid properties, such as the specific volume, are evaluated at the pump inlet conditions. The same modeling approach is applied to the water pump, which is required in certain configurations, such as for simulating an absorption heat transformer.

#### 2.4 Dynamic models

Up to this point, the dynamic models have been focus on the single effect absorption heat pump, which serves as the core component of the AHE. The dynamic model of the absorption heat pump is implemented in an object oriented manner, utilizing modular component models for pipes, valves, pumps, the solution heat exchanger, and the main

heat exchangers (i.e. absorber, generator, evaporator and condenser) among others.

Key modeling assumptions are summarized below. These assumptions are commonly adopted in the literature (Herold, Radermacher, and Klein 2016).

- The refrigerant is assumed to be pure water.
- The condenser and generator operate at the same pressure, as do the evaporator and absorber, i.e. no pressure loss between them is considered.

Some of the component models such as valves, pumps and the solution heat exchanger have already been introduced (see section 2.3). Additional models, including pipes and various auxiliary components (e.g. sources), are taken from the MSL (Modelica Association 2024).

The primary work in the dynamic modelling involve the main heat exchangers. Several modeling approaches have been implemented, with a key distinction related to how heat exchange between the internal and external fluids and thermal inertia is handled.

The simplest approach utilizes an internal heat exchanger and it is analog to the static model formulation, where a fixed UA values is defined and the heat transfer rate is calculated using the logarithmic mean temperature difference. The process dynamics in this model are mainly limited to inertia related to the inner volumes of the vessels. The alternative approach models the heat exchanger externally, using a discrezited structure. For comparison, models ending in \_heatport and \_internalHEX within the FluidBased.Dynamic.Components illustrate the effects of the difference package the modelling approach. More specifically, models AHPse\_Dyn\_internalHEX and AHPse Dyn heatport nocp within the package ... Components. Validation provide a direct contrast between these two approaches.

Within the external heat exchanger modeling strategy, several versions have been developed. These include models that account for the thermal capacity of the heat exchanger itself, such as ...Dynamic.AHP.AHP. Furthermore, some models are also capable of representing heat losses, whether radiative, convective, or both.

Some implementations incorporate a two-stage heat exchange process, with an additional heat exchanger between the external fluid and the entering solution in the absorber and generator; such models end in \_hex\_extended. This modification is motivated by the specific design of the AHP under study (WEGRACAL® SE 15), whose handbook indicates that the liquid solution coming from the absorber is evenly distributed within the generator and includes a sprayer in its schematics. A similar configuration is shown for the solution path from the absorber to the generator. In this context, incorporating an additional heat exchanger provides a straightforward way to reflect this design feature. However, it should be noted that the models do not include recirculation within

the heat exchanger, which would be required to faithfully model the evaporator. This represents a limitation of the current models.

Further extensions include configurations that incorporate an additional solution pump transferring fluid from the generator back to the absorber, as implemented in ...Dynamic.AHP\_AHP\_pump. This modification is again based on the WEGRACAL® SE 15 handbook, which explicitly states that the solution with a high lithium bromide concentration is pumped back to the absorber.

As with the static models, some code duplication exists in the current implementation, which complicates code review. This limitation will be addressed by introducing base classes and using the extends clause, by enabling feature toggling through if-conditioned component declarations. On the other hand, some of the dynamic models offer increased flexibility, compared to the static models, through the use of variable UA values in certain configurations, such as ...Dynamic.AHP.AHP\_hex\_extended. In summary, the different versions result from a step-bystep implementation process that progressively increased model complexity and incorporated specific design features of WEGRACAL® SE 15, the device employed for model validation purposes. A clear conclusion about which model is preferable cannot yet be drawn, as no detailed analysis comparing the versions in terms of results and performance has been conducted.

#### 2.4.1 Generator and Absorber

In general, the version with an externalized heat exchanger is preferred due to its greater flexibility. This modeling approach is applied to both the generator and the absorber, which are described in more detail below.

The same general modeling strategy is used to model the absorber and the generator. The main differences them lie in the direction of the vapor flow (compare the flow at position 7 and 10) and in the thermodynamic states of the entering fluid streams, see for example, the differences between the states at position 3 and 6 (refer to Figure 4).

The internal mass balance equations define the total mass within the component as the sum of the vapor and liquid phase masses. The total must equal the combined mass of refrigerant and lithium bromide solution, as formulated in Equations (8) to (10).

$$m = m_{ref} + m_{LiBr} = m_v + m_l \tag{8}$$

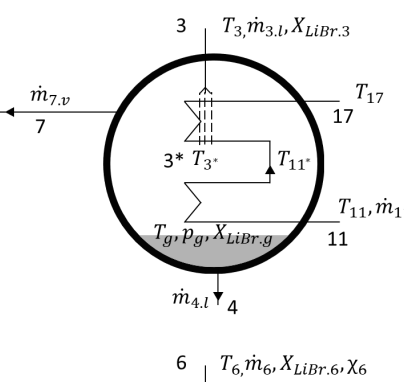
$$m_{ref} = m_v + m_l \cdot (1 - X_{LiBr}) \tag{9}$$

$$m_{LiBr} = m_l \cdot X_{LiBr} \tag{10}$$

The total mass is contained in a vessel of volume V, which is composed of contributions from both the vapor and liquid phases.

$$V = \frac{m_{\nu}}{\rho_{\nu}} + \frac{m_l}{\rho_l} \tag{11}$$

A vapor-liquid equilibrium is assumed between the liquid phase (H<sub>2</sub>O/LiBr solution) and the vapor phase (pure



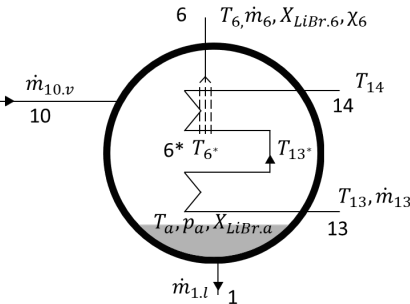


**Figure 4.** Schematics of the generator (top) and absorber (bottom).

refrigerant). Phase equilibrium is maintained by requiring the chemical potential of water to be equal in both phases, as expressed in Equation (12).

$$\mu_{l.ref} = \mu_{v} \tag{12}$$

The mass balance for the refrigerant in the generator and absorber is described by Equations (13) and (14) respectively. For example, the change in refrigerant mass within the generator is determined by the net mass flow: it is equal to the mass flow rate of the refrigerant entering from the absorber  $\dot{m}_{3.ref}$ , minus the mass flow rate of vaporized refrigerant exiting into the condenser  $\dot{m}_{7.v}$ , and minus the portion of liquid refrigerant returned from the generator to the absorber  $\dot{m}_{4.l.ref}$ .

$$\frac{d(m_{g.ref})}{dt} = \dot{m}_{3.l.ref} - \dot{m}_{7.v} - \dot{m}_{4.l.ref}$$
 (13)

$$\frac{d(m_{a.ref})}{dt} = \dot{m}_{6.l.ref} + \dot{m}_{10.v} - \dot{m}_{1.l.ref}$$
 (14)

Similarly, the mass balance for the solution in the generator and absorber is described by Equations (15) and (16) respectively.

$$\frac{d(m_{g.LiBr})}{dt} = \dot{m}_{3.l.LiBr} - \dot{m}_{4.l.LiBr} \tag{15}$$

$$\frac{d(m_{a.LiBr})}{dt} = \dot{m}_{6.l.LiBr} - \dot{m}_{1.l.LiBr}$$
 (16)

With respect to the energy balance, the mass within the generator gains energy from three main sources: heat transfer from the external fluid, which provides the driving heat for refrigerant vaporization  $\dot{Q}_g$ , heat exchange with the surroundings, accounting for possible heat losses or gains  $\dot{Q}_{g.loss}$  and enthalpy carried by the mass flows  $\dot{H}_g$ . The corresponding energy balance is defined by Equation (17).

$$\frac{d(U_j)}{dt} = \dot{H}_j + \dot{Q}_j - \dot{Q}_{loss.j} \quad \text{where } j \in \{g, a\}$$
 (17)

The heat losses or gains to the environment are modelled using a constant thermal conductance and are assumed to be proportional to the temperature difference between the internal temperature of the vapor liquid equilibrium mixture, denoted as  $T_g$  for the generator and  $T_a$  for the absorber, and the ambient temperature  $T_{amb}$  ( $T_{amb}$  is now fixed to 25°C). This relationship is defined by Equation (18).

$$\dot{Q}_{loss,j} = UA_{j,amb} \cdot (T_j - T_{amb})$$
 where  $j \in \{g, a\}$  (18)

The contribution of the enthalpy flow rate  $\dot{H}$  to the energy balance in the generator and absorber is defined by Equations (19) and (20) respectively. It is expressed as the sum of enthalpy flows, i.e. the product of each entering (positive) and leaving (negative) mass streams and their respective associated specific enthalpies.

$$\dot{H}_g = \dot{m}_{3.l} \cdot h_{3^*.l} - \dot{m}_{7.\nu} \cdot h_{7.\nu} - \dot{m}_{4.l} \cdot h_{4.l}$$
 (19)

$$\dot{H}_a = \dot{m}_6 \cdot h_{6^*} + \dot{m}_{10,\nu} \cdot h_{10,\nu} - \dot{m}_{1,l} \cdot h_{1,l}$$
 (20)

Note that the enthalpies  $h_{3^*.l}$  and  $h_{6^*.l}$  correspond to the thermodynamic states at positions  $3^*$  and  $6^*$  respectively. These represent the "pre-heated" and "pre-cooled" streams, i.e. streams that have already exchanged heat with the external fluid. As a result, the heat transfer from the external fluid to the vessel contents is modeled in two stages.

The first stage involves heat transfer between the incoming external fluid (at position 11 and 13) and the internal vapor-liquid mixture within the generator or absorber, maintained at temperature  $T_g$  or  $T_a$ . The second stage involves heat exchange between the cooled external fluid (at positions 11\* and 13\*) and the fluid entering from the external circuit, initially at temperature  $T_3$  or  $T_6$ , which is then heated and cooled to  $T_{3^*}$  and  $T_{6^*}$  respectively. This additional heat transfer step is specific to model versions identified by the suffix hex\_extended.

The first stage corresponds to the main heat exchanger. In this model, the thermal capacity of the solid structure of the heat exchanger is explicitly considered. Both the external fluid and the solid parts are spatially discretized into n elements to capture transient behavior accurately (see Figure 5). The total heat flow entering the generator and absorber is defined by Equation (21).

$$\dot{Q}_j = \sum_{n=1}^n UA_j \cdot (T_{j.s.i} - T_j) \quad \text{where } j \in \{g, a\}$$
 (21)

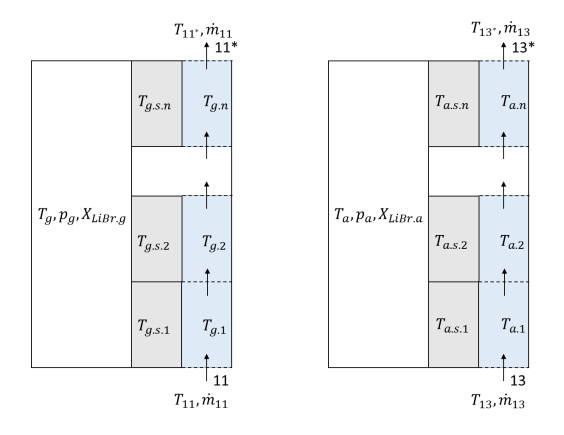


**Figure 5.** Schematics of internal heat exchanger model of generator (left) and absorber (right).

The energy balance of the solid part of the heat exchanger is defined by Equation (22) for each discretized section i. Here, C denotes the heat capacity of the solid in each section, expressed in Joules per Kelvin, and is calculated as  $C = c \cdot m$ , where c is the specific heat capacity and m is the mass of the solid in the corresponding section.

$$C\frac{d(T_{j.s.i})}{dt} = UA_j \cdot (T_j - T_{j.s.i}) + UA_j \cdot (T_{j.i} - T_{j.s.i})$$
 (22)

where  $j \in \{g, a\}$  and  $i \in \{1, 2, ..., n\}$ 

The external fluid is modeled using the DynamicPipe model of the MSL. The static head is set to zero. The pressure loss coefficients are set to a negligible value. Changes in density are expected to be low. The energy balance equations for the external fluid are defined by Equations (23) and (24).  $\dot{m}_{j.ext}$  and  $h_{j.i}$  are used to indicate the entering (in) and leaving (out) mass flow rate and specific enthalpy at each volume i.

$$\frac{d(U_{j,i})}{dt} = \dot{H}_{j,i.ext} - UA_j \cdot (T_{j,i} - T_{j,s,i})$$
 (23)

$$\dot{H}_{i,ext} = \dot{m}_{i,ext,in} \cdot h_{i,i,in} - \dot{m}_{i,ext,out} \cdot h_{i,i,out}$$
 (24)

where  $j \in \{g, a\}$  and  $i \in \{1, 2, ..., n\}$ 

With regard to the second stage of heat transfer from the external fluid to the entering fluid at the main vessel, represented by  $\dot{Q}_{hex}$ , (corresponding to positions 11\*, 17, 3 and 3\* for the generator, and positions 13\*, 14, 6 and 6\* for the absorber), it is important to note that the thermal capacity of the solid structure is neglected in this part of the model. The model used is based on PartialEffectivenessNTU<sup>1</sup>. In this model, the overall heat transfer coefficient-area product (UA value) is assumed to be constant. The heat transfer is defined as the product of the maximum possible heat flow rate  $\dot{Q}_{hex.max}$ 

and the heat exchanger effectiveness  $\varepsilon$ , as shown in Equation (25). The effectiveness  $\varepsilon$  is a function of the number of transfer units ( $NTU = UA/\dot{C}_{min}$ ) and the thermal capacities of the internal and external streams,  $\dot{C}_{int}$  and  $\dot{C}_{ext}$ , respectively, where  $\dot{C} = \dot{m} \cdot c_p$ . More specifically,  $\varepsilon$  depends on the ratio of the minimum to the maximum capacity rate,  $\dot{C}_r = min(\dot{C}_{int}, \dot{C}_{ext})/max(\dot{C}_{int}, \dot{C}_{ext})$ , as described in Equation (26). The maximum possible heat transfer rate  $\dot{Q}_{hex.max}$  is defined as the product of the minimum thermal capacity rate and the temperature difference between the two entering fluid streams (e.g. temperatures at position 11\* and 3 in the case of the generator), as shown in Equation (27).

$$\dot{Q}_{hex} = \dot{Q}_{hex\ max} \cdot \varepsilon \tag{25}$$

$$\varepsilon = \frac{1 - e^{-NTU \cdot (1 - \dot{C}_r)}}{1 - \dot{C}_r \cdot e^{-NTU \cdot (1 - \dot{C}_r)}} \tag{26}$$

$$\dot{Q}_{hex.max} = \dot{C}_{min} \cdot (T_i - T_k) \tag{27}$$

where  $(j,k) \in \{(11^*,3),(13^*,6)\}$ 

## 2.4.2 Evaporator and condenser

The primary difference in the modeling of the evaporator and condenser, compared to the generator and absorber, lies in the treatment of heat transfer and the working fluid. In the evaporator and condenser, only pure refrigerant is present, and the heat exchange between the vapor–liquid equilibrium mixture and the external fluid is modeled in a simplified manner. Specifically, only a single main heat exchanger is used in these components—no extended or two-stage heat exchanger configuration is applied.

The equations that describe the mass balance of the evaporator and condenser are equivalent to Equations (8) to (12) assuming  $X_{LiBr} = 0$ . Equations (13) and (14) need to be substituted by Equations (28) and (29).

$$\frac{d(m_{c.ref})}{dt} = \dot{m}_{7.v.ref} - \dot{m}_{8.l.ref}$$
 (28)

$$\frac{d(m_{e.ref})}{dt} = \dot{m}_{9.l.ref} + \dot{m}_{9.v.ref} - \dot{m}_{10.v.ref}$$
 (29)

Regarding the energy balance, Equations (18), (22), and (23) apply under the assumption that  $j \in \{c, e\}$ . Furthermore, Equations (19) and (20) must be replaced by Equations (30) and (31).

$$\dot{H}_c = \dot{m}_{7,v} \cdot h_{7,v} - \dot{m}_{8,l} \cdot h_{8,l} \tag{30}$$

$$\dot{H}_e = \dot{m}_9 \cdot h_9 - \dot{m}_{10,\nu} \cdot h_{10,\nu} \tag{31}$$

As mentioned above, the two-stage heat exchanger configuration is not applied in this case. Consequently, Equations (25) to (27) are not relevant to the evaporator and condenser models.

<sup>&</sup>lt;sup>1</sup>Model Fluid.HeatExchangers.BaseClasses.PartialEffectivenessNTU of the Buildings library (Wetter et al. 2014)

# 3 Absorption heat exchanger (AHE) model validation

## 3.1 Model description

An AHE model has been developed based on the PlateHeatExchangerEffectivenessNTU model for the external heat exchanger and the Dynamic.AHP.AHP\_pump\_hex\_extended model for the AHP. This model has been validated using experimental measurements obtained within the framework of the Absolut project (Eberhöfer 2022; Zotter, Eberhöfer, and Seidnitzer-Gallien 2023). For detailed information about the experimental test rig, the reader is referred to (Eberhöfer 2022).

The measurement data are used as input for the model, particularly the inlet mass flow rates and temperatures at the absorber, external heat exchanger, and generator. These measurements correspond to the sensor locations at positions 13, 20, and 11, respectively (see Figure 1).

In regard of the parametrization and setup,

- Based on estimation heat loss coefficients from (Eberhöfer 2022), the parameter U\_amb is fixed to 3 W/K for each main heat exchanger. Heat losses due to radiation are not considered.
- Details on the internal control of the absorption heat pump (e.g. solution pump) are not known. The mass flow rate from the generator to the absorber has been fixed to 0.12 kg/s. The mass flow rate from the absorber to the generator is adjusted to keep the volume at the generator at a constant level.
- The volume of each vessel is estimated to be 70 liters.
- The sum of heat capacity per section C used in Equation 22 is set to 5 kJ/K for all main heat exchangers. The values in Table 1 of (Kohlenbach and Ziegler 2008) are used as reference values. The values of the heat exchanger tube bundles (assuming 100% weight) vary from 3.9 kJ/K to 6.1 kJ/K.
- The external heat exchanger SWEP B25Tx41/2P is parametrized directly based on expected performance obtained with the manufacturer software.

In regard of the model calibration, the main work is related to the estimation of appropriate values for the 6 unknown UA values of the AHP heat exchangers. The calibration is performed manually through stepwise adaptation of the parameters, using approximately 90 stationary points from various experiments as benchmarks. The UA value for each element n required for Equation (22), which are the same values used in Equation (23) are obtained with Equation (32) and are defined based on nominal operating conditions by two parameters ( $\dot{m}_{nom}$  and  $UA_{nom}$ ). The mass flow rates  $\dot{m}$  and  $\dot{m}_{nom}$  are referred to the external fluid, i.e. positions 11, 13, 16 and 18.

$$UA_j = \frac{UA_{nom}}{n} \left(\frac{\dot{m}}{\dot{m}_{nom}}\right)^{0.6} \quad \text{where } j \in \{g, a\}$$
 (32)

The values after calibration are summarized in Table 1. Additionally, the fixed UA in W/K values used for the solution heat exchanger, and the second stage heat exchange at the generator and absorber, see Equations (25) to (27), are set respectively to 350, 100 and 400 W/K.

**Table 1.** Parametrization of main heat exchangers after calibration.

Heat exchanger	UA <sub>nom</sub> in kW/K	<i>ṁ</i> <sub>nom</sub> in kg/s
Evaporator	1.2	0.045
Generator	1.5	0.045
Absorber	3.9	0.35
Condenser	3.9	0.35

To analyze the dynamic behavior of the model, simulation results covering 14 hours of experimental operation are compared with measurement data. The measurement uncertainty of the temperature sensors is estimated at  $\pm$  0.2 K as reported in (Zotter, Eberhöfer, and Seidnitzer-Gallien 2023). The comparison primarily focuses on the outlet temperatures of the main heat exchangers. To assess the model's accuracy under steady-state conditions, data points identified as quasi-stationary- according to the criteria outlined in (Eberhöfer 2022) are used. These points correspond to periods in which the system operation is assumed to have stabilized.

Results from a single experimental run are presented here. The boundary conditions used in the simulation are summarized in Figure 6. Points at which the operation is considered to have reached steady-state are marked with circles. For this analysis, the evaluation period spans from hour 1 to hour 15 of regular operation.

#### 3.2 Validation results

Simulation results at positions 12, 14, 15, 17, 19 and 21 (see Figure 1) over the evaluation period of the experiment are presented in Figure 7 alongside the corresponding measurement data and the calculated deviations. The model predicts the outlet temperature behavior with generally good accuracy. A total of 841 values (one every minute) are used for calculate the deviation at the given instant and used for the evaluation, see Table 2. Most monitored temperatures, specifically  $T_{14}$ ,  $T_{15}$ ,  $T_{17}$ , and  $T_{21}$ , show low average deviations in the range of -0.4 K to 1.3 K, with deviations spanning from -2.7 K up to 3.2 K. In contrast, the outlet temperature of the external heat exchanger  $T_{19}$  and the outlet temperature of the evaporator  $T_{12}$  exhibit a higher average deviation of 2.7 K and 1.6 K with a maximum deviation (underestimated temperature) of 8.3 K and 3.1 K respectively.

When evaluating temperature deviations under steadystate operating conditions, the average deviations are comparable to those observed over the entire duration of the

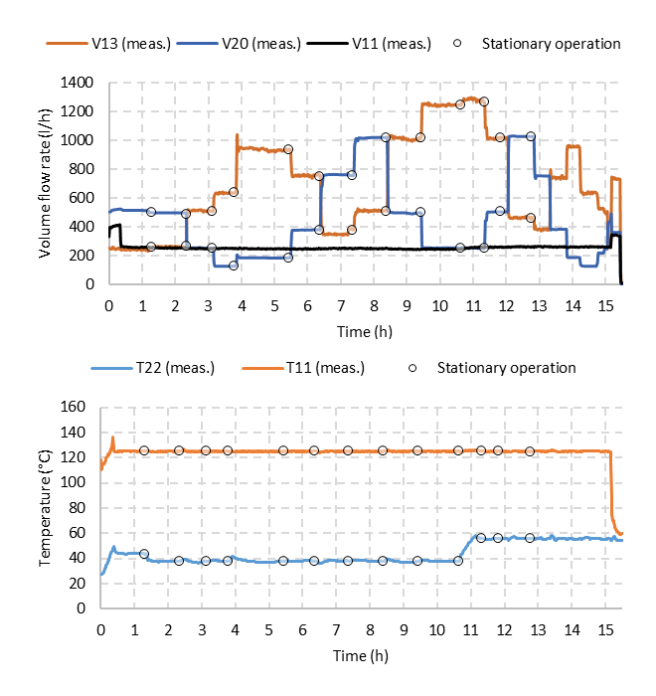


**Figure 6.** Measured data (meas.) used as boundary conditions for the model validation. Volume flow rates (top) and temperatures (bottom). Volume flow rate and temperature entering the generator  $V_{11}$  and  $T_{11}$ . Volume flow rate entering the absorber  $V_{13}$  and the external heat exchanger (secondary side)  $V_{20}$  and their temperature  $T_{22}$ .

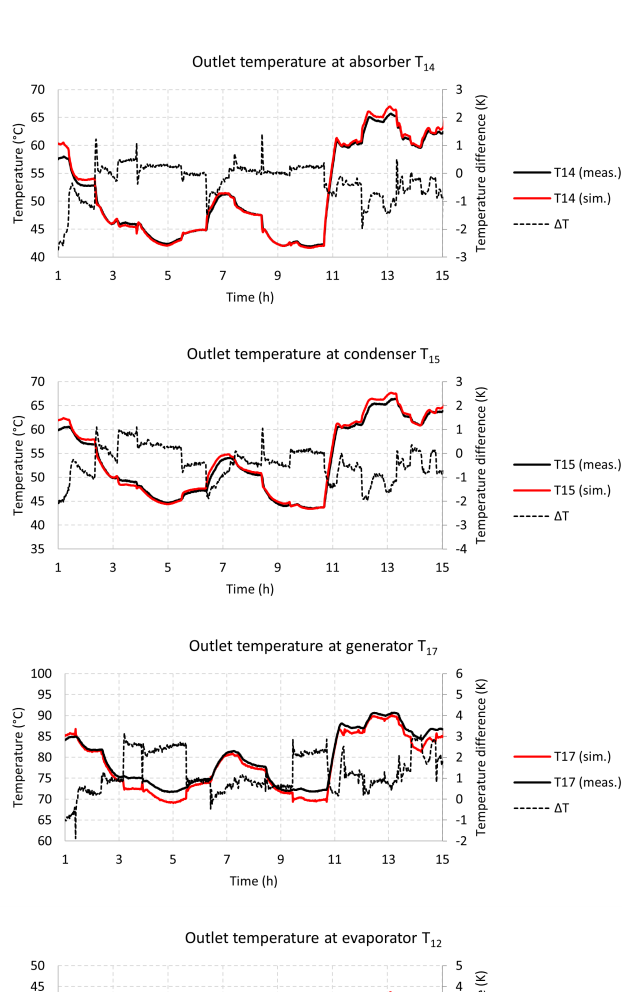
experiment (cf. Table 2 and Table 3). It is noteworthy that the large temperature deviations previously observed at the external heat exchanger outlet ( $T_{19}$ ) during transient conditions are reduced once the system reaches steady-state. Under these conditions, the deviations at  $T_{19}$  range from a minimum of 0.74 K to a maximum of 5.5 K, with an average deviation of 2.6 K across the thirteen steady-state data points - the highest average deviation among the six evaluated temperatures.

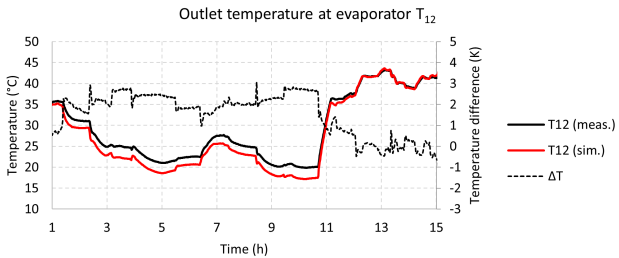
## 4 Conclusions

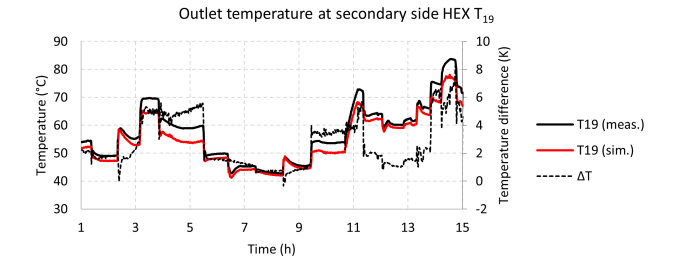
The presented Absolut Modelica library includes both static models, which have been verified against literature

**Table 2.** Average, maximum and minimum temperature deviations (in Kelvin) defined as the reference value (measurement) minus the calculated values (simulation result) for 14 hours evaluation period.

	Temperature deviation in K		
Temperature	Average	Maximal	Minimal
$T_{14}$	-0.26	1.42	-2.73
$T_{15}$	-0.39	1.1	-2.1
$T_{12}$	1.56	3.07	-0.59
$T_{17}$	1.28	3.16	-1.87
$T_{19}$	2.70	8.26	-0.33
$T_{21}$	-0.07	0.65	-1.38







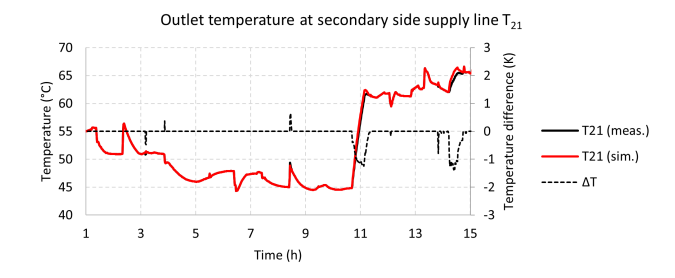


**Figure 7.** Temperature difference  $(\Delta T)$  in K between measurements (meas.) and simulation results (sim.) at outlet of main heat exchangers.

**Table 3.** Average, maximum and minimum temperature deviations (in Kelvin) defined as the reference value (measurement) minus the calculated values (simulation result) for monitored positions under steady-sate operating conditions.

	Temperature deviation in K		
Temperature	Average	Maximal	Minimal
$T_{14}$	-0.29	0.53	-2.11
$T_{15}$	-0.43	0.7	-1.66
$T_{12}$	1.2	2.61	-0.79
$T_{17}$	1.72	2.74	-0.01
$T_{19}$	2.58	5.49	0.74
$T_{21}$	0.0	0.0	-0.05

values and are suitable for preliminary analysis of absorption thermodynamic cycles, and dynamic models. Despite the current limitations - such as the use of simplified heat exchanger models and uncertainties related to internal control - the simulation results of the dynamic models show good agreement with experimental data. Both the dynamic and static models utilize the implemented correlations for the  $H_2O/LiBr$  working pair. Overall, the library provides a solid foundation for the analysis of absorption thermodynamic cycles, offering basic yet reliable models for further study and development. As an opensource resource (available at https://github.com/carlesRT/Absolut), it is intended to be extended and refined by the community to address current limitations and support broader applications.

# Acknowledgements

The project AbSolut (FFG-Nr.: 879433) is supported with the funds from the Climate and Energy Fund and implemented in the framework of the RTI-initiative "Flagship region Energy". The TREASURE project has received funding from the European Union under Grant Agreement No. 101136095. Views and opinions expressed are however those of the author(s) only and do not necessarily reflect those of the European Union or CINEA. Neither the European Union nor CINEA can be held responsible for them.



## References

Chen, J.J.J. (1987). "Comments on improvements on a replacement for the logarithmic mean". In: *Chemical Engineering Science* 42.10. Publisher: Elsevier BV, pp. 2488–2489.

## Nomenclature

Table 4. Description of subscripts and symbols

Table 4. Description of subscripts and symbols.			
Subscript	Description		
a	Absorber		
amb	Ambient / Surroundings		
c	Condenser		
e	Evaporator		
el	Electric		
ext	External fluid		
g	Generator		
$\stackrel{\circ}{h}$	Hydraulic		
hex	Heat exchanger		
l	Liquid state		
LiBr	Lithium bromide		
Loss	Heat losses		
max	Maximal		
min	Minimal		
p	constant pressure		
r	Ratio between minimal and maximal		
ref	Pure refrigerant		
S	Solid state		
sol	Solution, i.e. LiBr-water mixture/solution		
v	Vapor state		
1,2,3,	Position of the variable in the AHE		
Symbols	Description		
	<u> </u>		
C	Heat capacity (I/K)		
C Ċ	Heat capacity (J/K) Capacity rate (W/K)		
Ċ	Capacity rate (W/K)		
Ċ c	Capacity rate (W/K) Specific heat capacity (J/(kg.K))		
Ċ с Н	Capacity rate (W/K) Specific heat capacity (J/(kg.K)) Enthalpy flow rate (W)		
Ċ c Ĥ m	Capacity rate (W/K) Specific heat capacity (J/(kg.K)) Enthalpy flow rate (W) Mass (kg)		
Ċ c Ĥ m ṁ	Capacity rate (W/K) Specific heat capacity (J/(kg.K)) Enthalpy flow rate (W) Mass (kg) Mass flow rate (kg/s)		
Ċ c H m m NTU	Capacity rate (W/K) Specific heat capacity (J/(kg.K)) Enthalpy flow rate (W) Mass (kg) Mass flow rate (kg/s) Number of transfer units (-)		
Ċ c H m m TU	Capacity rate (W/K) Specific heat capacity (J/(kg.K)) Enthalpy flow rate (W) Mass (kg) Mass flow rate (kg/s) Number of transfer units (-) Pressure (Pa)		
Ċ c Ĥ m m NTU p	Capacity rate (W/K) Specific heat capacity (J/(kg.K)) Enthalpy flow rate (W) Mass (kg) Mass flow rate (kg/s) Number of transfer units (-) Pressure (Pa) Heat flow rate (W)		
Ċ c H m m m VTU p Q T	Capacity rate (W/K) Specific heat capacity (J/(kg.K)) Enthalpy flow rate (W) Mass (kg) Mass flow rate (kg/s) Number of transfer units (-) Pressure (Pa) Heat flow rate (W) Temperature (K)		
Ċ c Ĥ m m M NTU p Q T	Capacity rate (W/K) Specific heat capacity (J/(kg.K)) Enthalpy flow rate (W) Mass (kg) Mass flow rate (kg/s) Number of transfer units (-) Pressure (Pa) Heat flow rate (W) Temperature (K) Internal energy (J)		
Ċ c H m m NTU p Q T U UA	Capacity rate (W/K) Specific heat capacity (J/(kg.K)) Enthalpy flow rate (W) Mass (kg) Mass flow rate (kg/s) Number of transfer units (-) Pressure (Pa) Heat flow rate (W) Temperature (K) Internal energy (J) Heat transfer coefficient times area (W/K)		
Ċ c H m m NTU p Q T U UA	Capacity rate (W/K) Specific heat capacity (J/(kg.K)) Enthalpy flow rate (W) Mass (kg) Mass flow rate (kg/s) Number of transfer units (-) Pressure (Pa) Heat flow rate (W) Temperature (K) Internal energy (J) Heat transfer coefficient times area (W/K) Volume (m³)		
Ċ c H m m m NTU p Q T U UA V	Capacity rate (W/K) Specific heat capacity (J/(kg.K)) Enthalpy flow rate (W) Mass (kg) Mass flow rate (kg/s) Number of transfer units (-) Pressure (Pa) Heat flow rate (W) Temperature (K) Internal energy (J) Heat transfer coefficient times area (W/K) Volume (m³) Work (W)		
Ċ c H m m NTU p Q T U UA V W X	Capacity rate (W/K) Specific heat capacity (J/(kg.K)) Enthalpy flow rate (W) Mass (kg) Mass flow rate (kg/s) Number of transfer units (-) Pressure (Pa) Heat flow rate (W) Temperature (K) Internal energy (J) Heat transfer coefficient times area (W/K) Volume (m³) Work (W) Mass fraction (kg/kg)		
Ċ c H m m NTU p Q T U UA V W X y	Capacity rate (W/K) Specific heat capacity (J/(kg.K)) Enthalpy flow rate (W) Mass (kg) Mass flow rate (kg/s) Number of transfer units (-) Pressure (Pa) Heat flow rate (W) Temperature (K) Internal energy (J) Heat transfer coefficient times area (W/K) Volume (m³) Work (W) Mass fraction (kg/kg) Valve opening (-)		
Ċ c H m m m NTU p Q T U UA V W X y ε	Capacity rate (W/K) Specific heat capacity (J/(kg.K)) Enthalpy flow rate (W) Mass (kg) Mass flow rate (kg/s) Number of transfer units (-) Pressure (Pa) Heat flow rate (W) Temperature (K) Internal energy (J) Heat transfer coefficient times area (W/K) Volume (m³) Work (W) Mass fraction (kg/kg) Valve opening (-) Heat exchanger effectiveness/efficiency (-)		
Ċ c H m m m NTU p Q T U UA V W X y ε η	Capacity rate (W/K) Specific heat capacity (J/(kg.K)) Enthalpy flow rate (W) Mass (kg) Mass flow rate (kg/s) Number of transfer units (-) Pressure (Pa) Heat flow rate (W) Temperature (K) Internal energy (J) Heat transfer coefficient times area (W/K) Volume (m³) Work (W) Mass fraction (kg/kg) Valve opening (-) Heat exchanger effectiveness/efficiency (-) Pump efficiency (-)		
Ċ c H m m m NTU p Q T U UA V W X y ε η μ	Capacity rate (W/K) Specific heat capacity (J/(kg.K)) Enthalpy flow rate (W) Mass (kg) Mass flow rate (kg/s) Number of transfer units (-) Pressure (Pa) Heat flow rate (W) Temperature (K) Internal energy (J) Heat transfer coefficient times area (W/K) Volume (m³) Work (W) Mass fraction (kg/kg) Valve opening (-) Heat exchanger effectiveness/efficiency (-) Pump efficiency (-) Specific chemical potential (J/kg)		
Ċ c H m m m NTU p Q T U UA V W X y ε η μ ν	Capacity rate (W/K) Specific heat capacity (J/(kg.K)) Enthalpy flow rate (W) Mass (kg) Mass flow rate (kg/s) Number of transfer units (-) Pressure (Pa) Heat flow rate (W) Temperature (K) Internal energy (J) Heat transfer coefficient times area (W/K) Volume (m³) Work (W) Mass fraction (kg/kg) Valve opening (-) Heat exchanger effectiveness/efficiency (-) Pump efficiency (-) Specific chemical potential (J/kg) Specific volume (kg/m³)		
Ċ c H m m m NTU p Q T U UA V W X y ε η μ	Capacity rate (W/K) Specific heat capacity (J/(kg.K)) Enthalpy flow rate (W) Mass (kg) Mass flow rate (kg/s) Number of transfer units (-) Pressure (Pa) Heat flow rate (W) Temperature (K) Internal energy (J) Heat transfer coefficient times area (W/K) Volume (m³) Work (W) Mass fraction (kg/kg) Valve opening (-) Heat exchanger effectiveness/efficiency (-) Pump efficiency (-) Specific chemical potential (J/kg)		

ISSN: 0009-2509. DOI: 10.1016/0009-2509(87)80128-8. URL: https://linkinghub.elsevier.com/retrieve/pii/0009250987801288 (visited on 2025-05-01).

Corrales Ciganda, Jose Luis et al. (2016-06). "Thermodynamic cycle models for the development of absorption heat trans-

- formers for the process industry". In: *Heat Powered Cycles Conference*. University of Nottingham.
- Cudok, Falk (2021-03-15). "Gemeinsamkeiten und Unterschiede zwischen Wärmetransformator- und Wärmepumpenprozess". Doktor der Ingenieurwissenschaften. Berlin: TU Berlin. 147 pp. URL: https://doi.org/10.14279/depositonce-11730.
- De La Calle, Alberto et al. (2016-12). "Dynamic modeling and simulation of a double-effect absorption heat pump". In: *International Journal of Refrigeration* 72, pp. 171–191. ISSN: 01407007. DOI: 10.1016/j.ijrefrig.2016.07.018. URL: https://linkinghub.elsevier.com/retrieve/pii/S0140700716302298 (visited on 2023-12-20).
- *Dymola* (2024-04-19). Version 2024x Refresh 1. URL: https://www.3ds.com/products/catia/dymola.
- Eberhöfer, Damian (2022-10). Adaption und Untersuchung eines Absorptionswärmetauschers zur Rücklauftemperaturreduktion in Fernwärmenetzen.
- EDF LAB CHATOU PRISME Department (2024). *Thermosyspro*. Thermosyspro. url: https://thermosyspro.com/index.html.
- El Hefni, Baligh (2019). *Modeling and Simulation of Thermal Power Plants with ThermoSysPro: A Theoretical Introduction and a Practical Guide*. In collab. with Daniel Bouskela. Cham: Springer. 1 p. ISBN: 978-3-030-05105-1.
- Febres, Jesus et al. (2017). District Cooling Open Source Library (DCOL). Version 4.1. URL: https://zenodo.org/records/1215665.
- Fu, Lin et al. (2010-03). "A district heating system based on absorption heat exchange with CHP systems". In: Frontiers of Energy and Power Engineering in China 4.1, pp. 77–83. ISSN: 1673-7393, 1673-7504. DOI: 10.1007/s11708-010-0022-0. URL: http://link.springer.com/10.1007/s11708-010-0022-0 (visited on 2024-02-09).
- G. Beckmann, F. Schittl, G. Piringer, D. Rixrath, R. Krotil, J. Krail (2019-12-19). TeTra Thermische Energietransformation zur Wärme- und Kälteauskopplung sowie Effizienzsteigerung in Nah- und Fernwärmenetzen. Final report, p. 125.
- Herold, Keith E., Reinhard Radermacher, and Sanford A. Klein (2016). Absorption Chillers and Heat Pumps. Second edition. London New York; Boca Raton: CRC Press. 1 p. ISBN: 978-1-4987-1435-8. DOI: 10.1201/b19625.
- Hu, Tianle, Yi Jiang, and Xiaoyun Xie (2009). "A Novel District Heating Solution Based on Absorption Heat Exchanger(AHE) for Different Types of Cogeneration Plants".
  In: Proceedings of international sustainable energy conference ISEC 2018, Graz.
- Kohlenbach, P. and F. Ziegler (2008-03). "A dynamic simulation model for transient absorption chiller performance. Part I: The model". In: *International Journal of Refrigeration* 31.2, pp. 217–225. ISSN: 01407007. DOI: 10.1016/j.ijrefrig.2007. 06.009. URL: https://linkinghub.elsevier.com/retrieve/pii/S0140700707001181 (visited on 2023-12-20).
- Li, Yan et al. (2011-02). "A new type of district heating method with co-generation based on absorption heat exchange (co-ah cycle)". In: *Energy Conversion and Management* 52.2, pp. 1200–1207. ISSN: 01968904. DOI: 10.1016/j.enconman. 2010.09.015. URL: https://linkinghub.elsevier.com/retrieve/pii/S0196890410004176 (visited on 2024-02-09).
- Modelica Association (2024). *Modelica Standard Library*. URL: https://github.com/modelica/ModelicaStandardLibrary.

- Modelica Association (n.d.). *Modelica*. URL: https://modelica.org/.
- OpenModelica (2024-12-14). Version v.1.24.3. URL: https://openmodelica.org/.
- Pettersson, F. (2008-08). "Heat exchanger network design using geometric mean temperature difference". In: *Computers & Chemical Engineering* 32.8. Publisher: Elsevier BV, pp. 1726–1734. ISSN: 0098-1354. DOI: 10.1016/j.compchemeng.2007.08.015. URL: https://linkinghub.elsevier.com/retrieve/pii/S0098135407002256 (visited on 2025-05-01).
- TIL Suite (n.d.). Aachen. URL: https://tlk-energy.de/software/til-suite.
- Wernhart, Michael et al. (2022). "Vereinfachung von Absorptionskälteanlagen-Modellen". In.
- Wetter, Michael et al. (2014-07-04). "Modelica Buildings library". In: *Journal of Building Performance Simulation* 7.4, pp. 253–270. ISSN: 1940-1493, 1940-1507. DOI: 10.1080/19401493.2013.765506. URL: http://www.tandfonline.com/doi/abs/10.1080/19401493.2013.765506 (visited on 2024-12-06).
- Yang, Fang, Nico Mirl, and Fabian Schmid (2020). *Potenziale* von Absorptionswärmepumpe in zentralisierten Wärmeversorgungsnetzen, p. 79.
- Yuan, Zhe and Keith E. Herold (2005-07). "Thermodynamic Properties of Aqueous Lithium Bromide Using a Multiproperty Free Energy Correlation". In: *HVAC&R Research* 11.3, pp. 377–393. ISSN: 1078-9669, 1938-5587. DOI: 10.1080/10789669.2005.10391144. URL: https://www.tandfonline.com/doi/full/10.1080/10789669.2005.10391144 (visited on 2023-12-20).
- Zhang, Yin, Wenxing Shi, and Yinping Zhang (2014-02). "From heat exchanger to heat adaptor: Concept, analysis and application". In: *Applied Energy* 115, pp. 272–279. ISSN: 03062619. DOI: 10.1016/j.apenergy.2013.11.015. (Visited on 2024-12-14).
- Zotter, Gerald, Damian Eberhöfer, and Carina Seidnitzer-Gallien (2023). "An energetical, exergetical and experimental analysis of an absorption heat exchanger used as transfer substation in an already existing district heating grid". In: 14th IEA Heat Pump Conference. Chicago.

# Appendix A: Review of open source models

ThermoSysPro The library (EDF LAB CHA-TOU PRISME Department 2024; Hefni 2019) includes a model for an absorption chiller (AbsorptionRefrigeratorSystem). This model employs non-standardized interfaces rather than the standard Modelica fluid interface FluidPort, limiting compatibility with other Modelica libraries. model provides interfaces for the external fluids of the evaporator and generator, while the condenser and absorber are connected in series using idealized internal sources and sinks. This modeling approach restricts the flexibility of the model, requiring modifications for more generic applications. The H<sub>2</sub>O/LiBr fluid functions in Properties. WaterSolution are sufficient for using the provided model but are constrained to a few equations with ambiguous references to the underlying data.

The District Cooling Open-Source Library (DCOL) is an open-source library that provides parametric thermofluid dynamic models for components of District Cooling Systems (Febres et al. 2017). It includes two absorption chiller models: a standard model and a simplified version that eliminates the need for control signals for internal valves. Both models share core components, namely the absorber, evaporator, generator, condenser, and pump, and utilize standard interfaces based on the Modelica Standard Library (Modelica Association 2024). The models are dynamic, accounting for vessel volumes and the mass of heat exchangers. Several examples simulations are provided, the simplified model runs successfully, while the standard model fails to initialize. The library also implements fluid property functions for the H<sub>2</sub>O/LiBr working pair. However, inconsistencies have been observed in the definition of some thermodynamic functions, particularly a mismatch that can lead to numerical issues. For example, given a pressure p, temperature T and concentration X the temperature(setState\_phX(p,h,X)), where the enthalpy obtained h is specificEnthalpy(setState\_pTX(p,T,X)) will differ slightly from the original input temperature T.

The Buildings library (Wetter et al. 2014) includes a model of an indirect steam-heated absorption chiller, that uses performance curves and is adapted from the EnergyPlus Absorption:Indirect model<sup>1</sup>. It employs standard interfaces from the Modelica Standard Library (Modelica Association 2024). The model uses six functions to predict key performance metrics, including cooling capacity, pump power consumption, generator heat flow rate, and condenser heat flow. These functions rely on performance data stored in a record. Several example simulations are provided to demonstrate the model's functionality.

# Appendix B: Additional validation results

In this section validation results of selected static models are presented. The results are used to confirm the correct implementation of the models and, indirectly, that of the fluid property correlations as well.

**Table 5.** Validation results for a single-effect absorption heat pump static model. Deviation in kW and % between reference values from Table 6.1 in (Herold, Radermacher, and Klein 2016) and the simulation results from AHP\_se\_UAfix\_eps.

	Deviation	
Heat flow rate at	in kW	in %
Absorber	0.09	0.62
Generator	0.09	0.62
Evaporator	0.07	0.61
Condenser	0.07	0.60
Solution heat exchanger	-0.03	-0.84

<sup>&</sup>lt;sup>1</sup>Chiller:Absorption:Indirect, https://designbuilder.co.uk

**Table 6.** Validation results for a single-effect Type II absorption heat pump static model. Deviation in kW and % between reference values from Table 6.6 in (Herold, Radermacher, and Klein 2016) and the simulation results from AHPTypeII\_UAfix\_HXeps.

	Deviation	
Heat flow rate at	in kW	in %
Absorber	-0.41	-0.22
Generator	-0.94	-0.51
Evaporator	0.10	0.05
Condenser	1.31	0.70
Solution heat exchanger	-0.33	-0.47

**Table 7.** Validation results of a static model for a parallel flow double-effect absorption heat pump. Deviation in kW and % between reference values from Table 7.4 in (Herold, Radermacher, and Klein 2016) and the simulation results from AHP\_pf\_de\_UAfix.

	Deviation	
Heat flow rate at	in kW	in %
Evaporator	-1.02	-0.28
Absorber	0.91	0.21
Condenser 1 (low pressure)	0.61	0.33
Condenser 2 / Generator 1	0.46	0.23
Generator 2 (high pressure)	-0.43	-0.16
Solution heat exchanger 1	-0.08	-0.25
Solution heat exchanger 2	0.04	0.06

**Table 8.** Validation results of a static model for a series flow double-effect absorption heat pump. Deviation in kW and % between reference values from Table 7.5 in (Herold, Radermacher, and Klein 2016) and the simulation results from AHP\_sf\_de\_UAfix.

	Deviation	
Heat flow rate at	in kW	in %
Evaporator	-17.02	-4.57
Absorber	21.21	4.62
Condenser 1 (low pressure)	6.08	2.84
Condenser 2 / Generator 1	10.91	5.88
Generator 2 (high pressure)	-10.22	-3.41
Solution heat exchanger 1	1.14	3.20
Solution heat exchanger 2	-1.24	-1.36

**Table 9.** Validation results of a static model for a resorption cycle. Deviation in kW and % between reference values from Table 8.6 in (Herold, Radermacher, and Klein 2016) and the simulation results from Resorption.

	Dev	Deviation	
Heat flow rate at	in W	in %	
Generator 1 (high pressure)	1.3	0.01	
Generator 2 (low pressure)	-1.2	-0.02	
Absorber 2 (high pressure)	0.1	0.00	
Absorber 1 (low pressure)	0.6	0.00	
Solution heat exchanger 1	-3.6	-0.10	
Solution heat exchanger 2	-1.6	-0.05	